Antenna above the Body

EM model

For the purpose of the electromagnetic simulation antenna is placed above a 3-layer half space representing a human body. Thickness and electrical properties of the layers (skin, fat, and muscle) are chosen to be the same as with Organization #3 (SCAU).

First, the current distribution along the wire is calculated, where the influence of the lossy, 3-layered half space is taken into account through the Fressnel Reflection Coefficient (RFC) approximation in the kernel of the Green's function. Next, transmitted electric field in arbitrary point inside the tissue is calculated by integrating the current along the wire and using Fressnel Transmission Coefficient approach. Calculation domain is limited to the cube of 50x50x20 mm with the resolution of 0.25 mm (Figure 6).

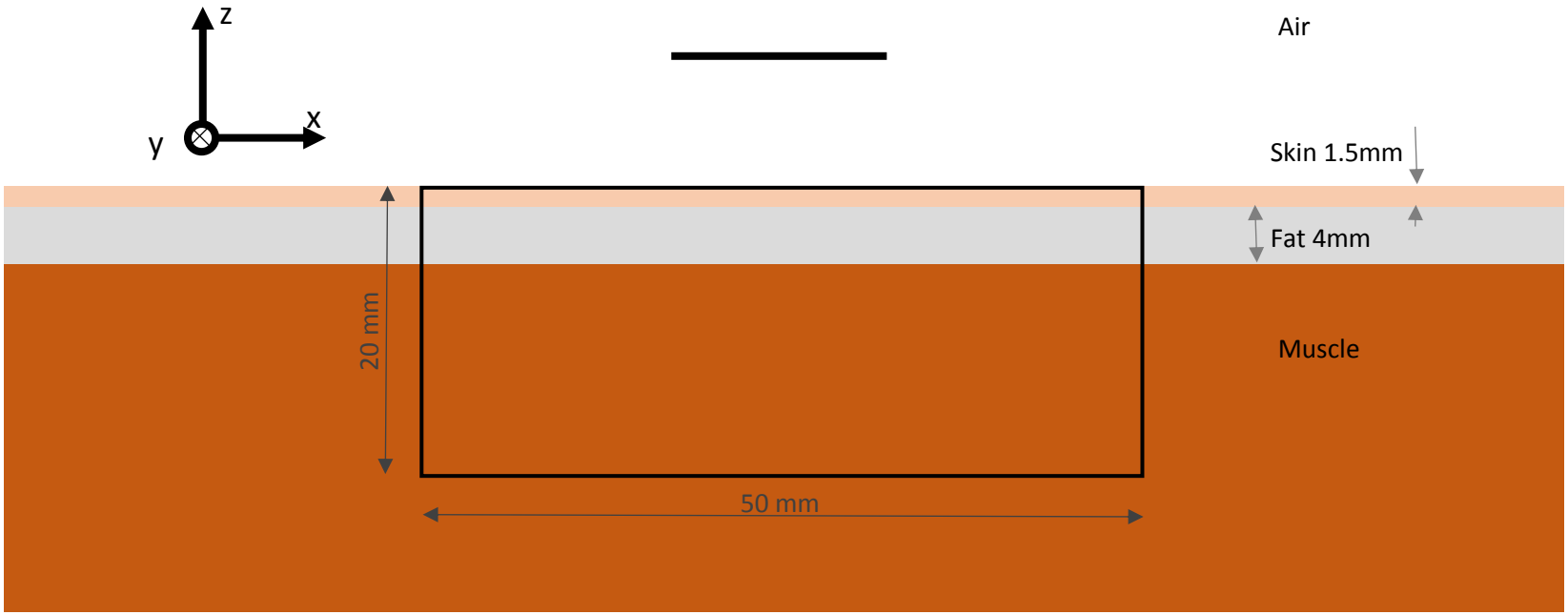

Figure 6: Body model and computational domain.

Table 3 – Tissue dielectric properties.

Tissue	10 GHz		30 GHz		60 GHz		90 GHz	
	σ (S/m)	ϵ_r	σ (S/m)	ϵ_r	σ (S/m)	ϵ_r	σ (S/m)	ϵ_r
skin	8.4824	32.409	27.31	16.63	37.96	9.096	41.94	6.826
fat	0.585	4.602	1.794	3.639	2.815	3.132	3.411	2.931
muscle	10.63	42.76	35.49	23.16	52.83	12.86	60.72	9.304

Thermal model

Electric field distribution calculated by the EM model are used as input parameters for the thermal model which is based on the Finite Element Method approach for solving steady state bioheat equation:

$$\nabla \cdot (k\nabla T) + B(T_a - T) + A + \rho\, SAR = 0 \qquad (1)$$

The heat transfer coefficient *h* between the skin and air was set to 10 W/(m^2 · °C). The air and body core temperature of T_{air} and T_b were set to 20 °C and 37 °C, respectively. All the other BCs were set to adiabatic. Tissue thermal properties were taken by [Sasaki2017] (same as Organization #1) and are summarized in Table 4.

On the surface of the sample the Neumann boundary condition is imposed:

$$k\frac{\partial T}{\partial \vec{n}} = -h_c(T - T_{air}) \qquad (2)$$

Assuming that heat transfer coefficient k is piecewise constant the weak form is obtained from differential equation (1) using standard Galerkin procedure:

$$\int_V [k\nabla N_i \cdot \nabla T + N_i B T]\, dV = \int_V N_i(B\, T_a + A + \rho SAR)\, dV + \oint_{\partial V} k\, N_i \nabla T \cdot d\vec{S} \qquad (3)$$

where N_i is the shape function that comes from discretization of volume V into set of tetrahedrons, ∂V is the surface bounding volume V and $d\vec{S}$ is the differential surface element of the volume ∂V. Equation (3), when combined with boundary condition (2) yields:

$$\int_V [k\nabla N_i \cdot \nabla T + N_i BT]\, dV = \int_V N_i(B\, T_a + A + \rho SAR)\, dV - \oint_{\partial V} k\, N_i h_c (T - T_{air}) dS \quad (4)$$

By expanding the temperature field into sum:

$$T = \sum_j N_j T_j \quad (5)$$

and implementing the standard FEM approach the matrix equation is obtained:

$$[A]\{T\} = \{b\} \quad (6)$$

By solving the matrix equation (6) the temperature field is obtained for the sample illuminated by dipole antenna.

Table 4 – Thermal parameters used by organization #5.

Parameter	Skin	Fat	Muscle
κ (W (m°C)$^{-1}$)	0.42	0.25	0.50
ρ (kg m^{-3})	1109	911	1090
A (W m^{-3})	1620	300	480
B (W (m°C)$^{-1}$)	9100	1700	2700

Obtained temperature increase distributions are shown in figures 7 to 10, alongside incident power densities. Maximum values of temperature increase and corresponding heating factors are given in table 5. Finally, graphical representation of calculated Heating factors is given in Figure 11.

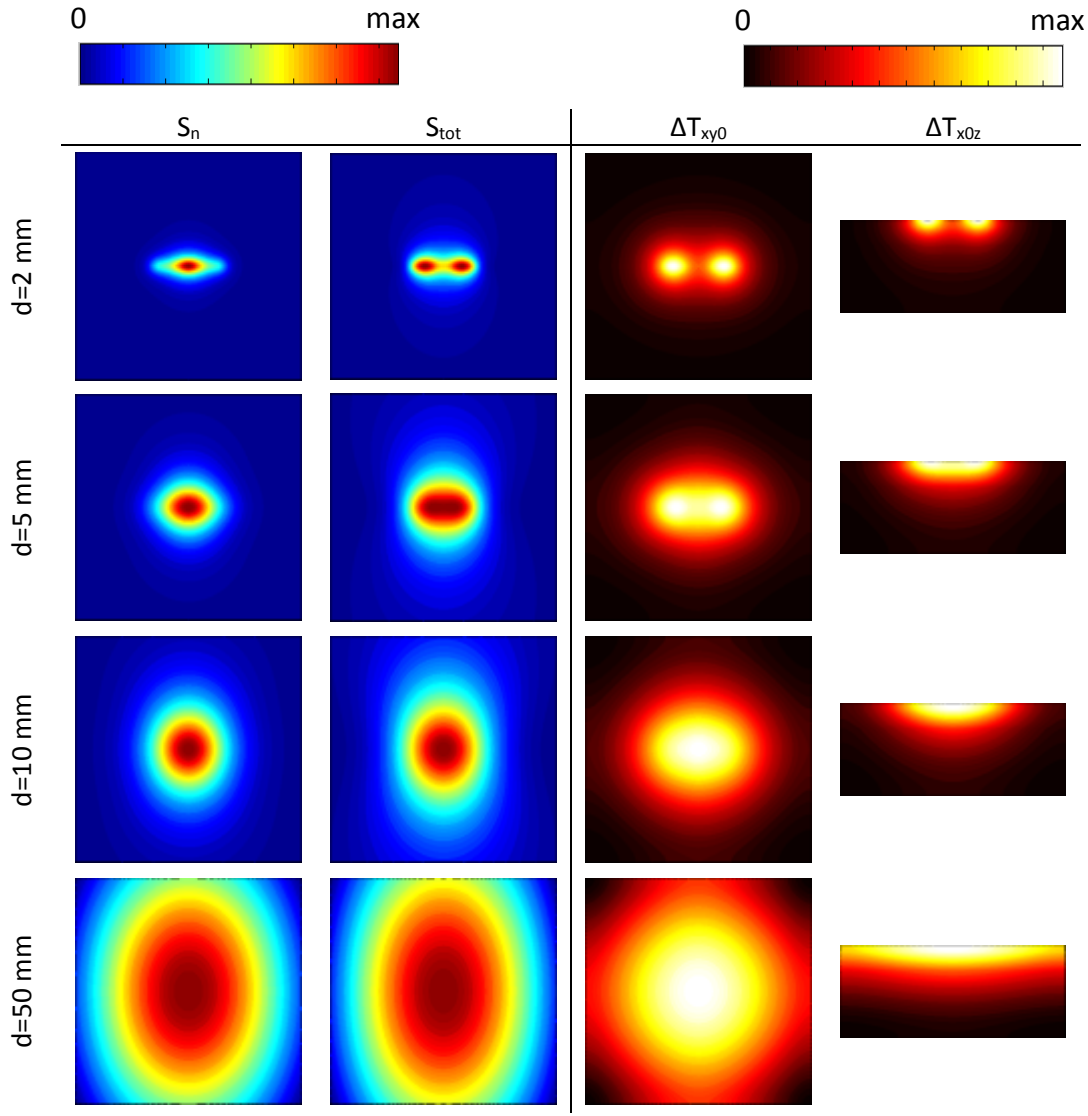

Figure 7: Power density and temperature distribution for the dipole at 10 GHz.

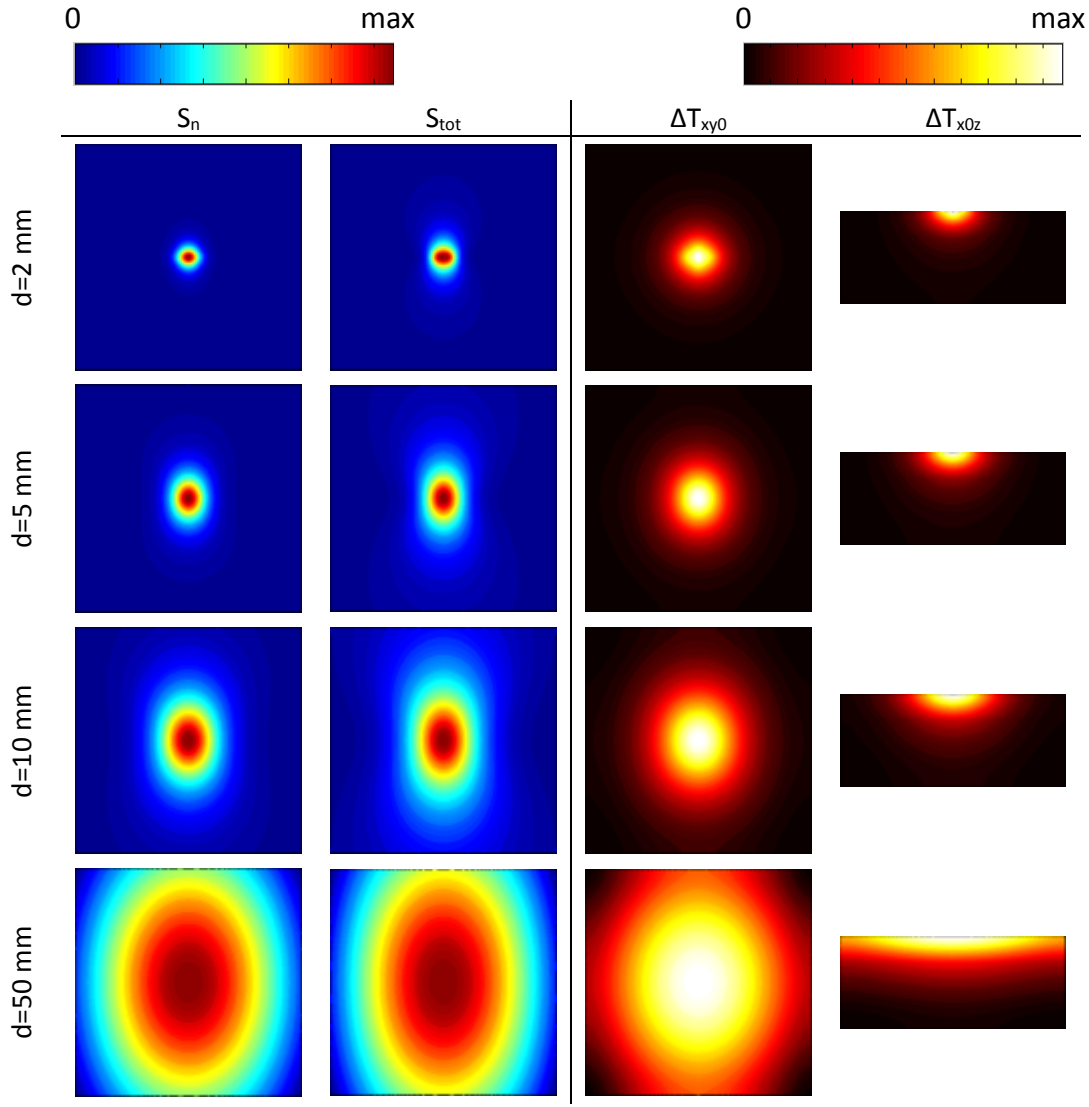

Figure 8: Power density and temperature distribution for the dipole at 30 GHz.

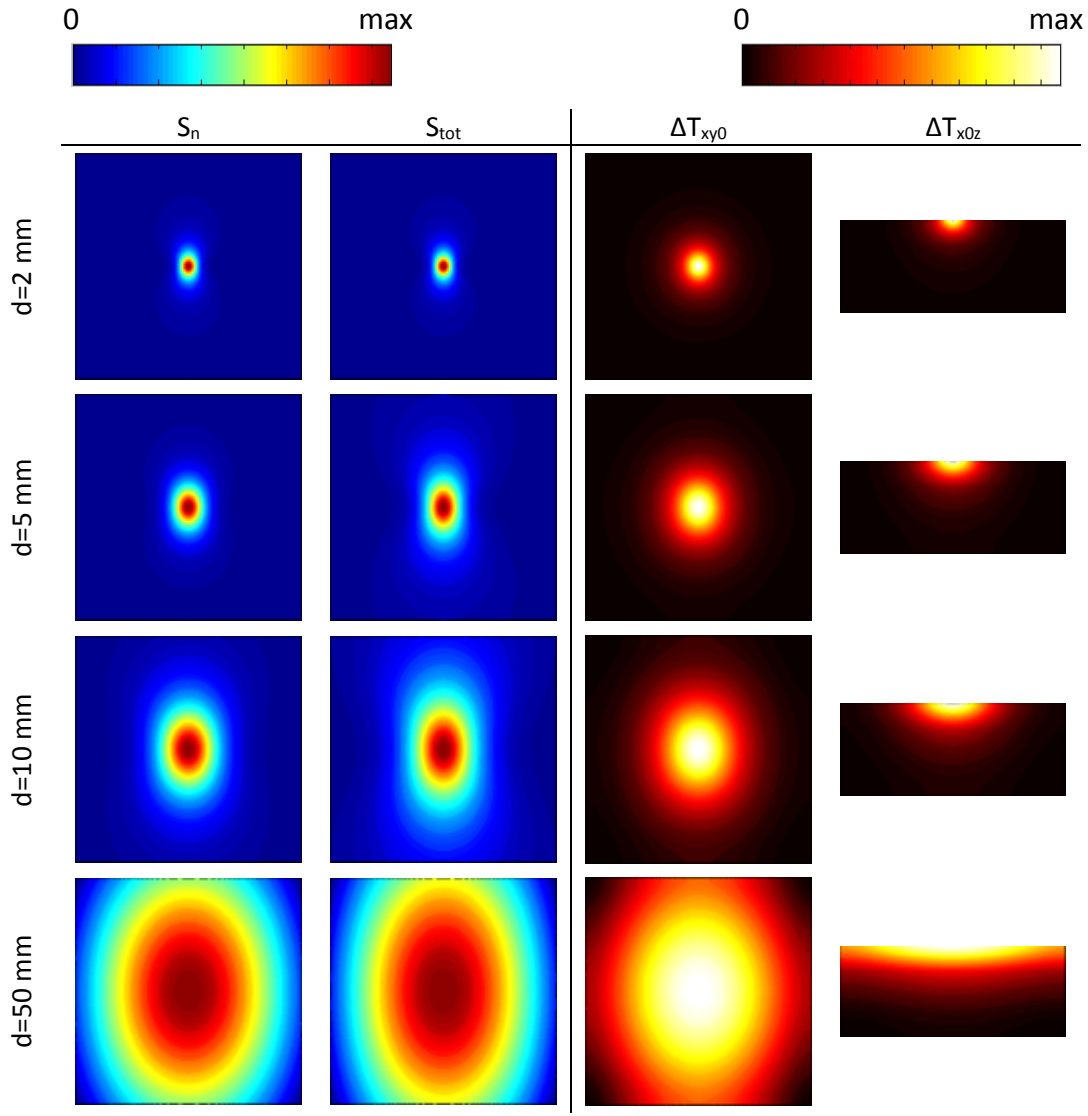

Figure 9: Power density and temperature distribution for the dipole at 60 GHz.

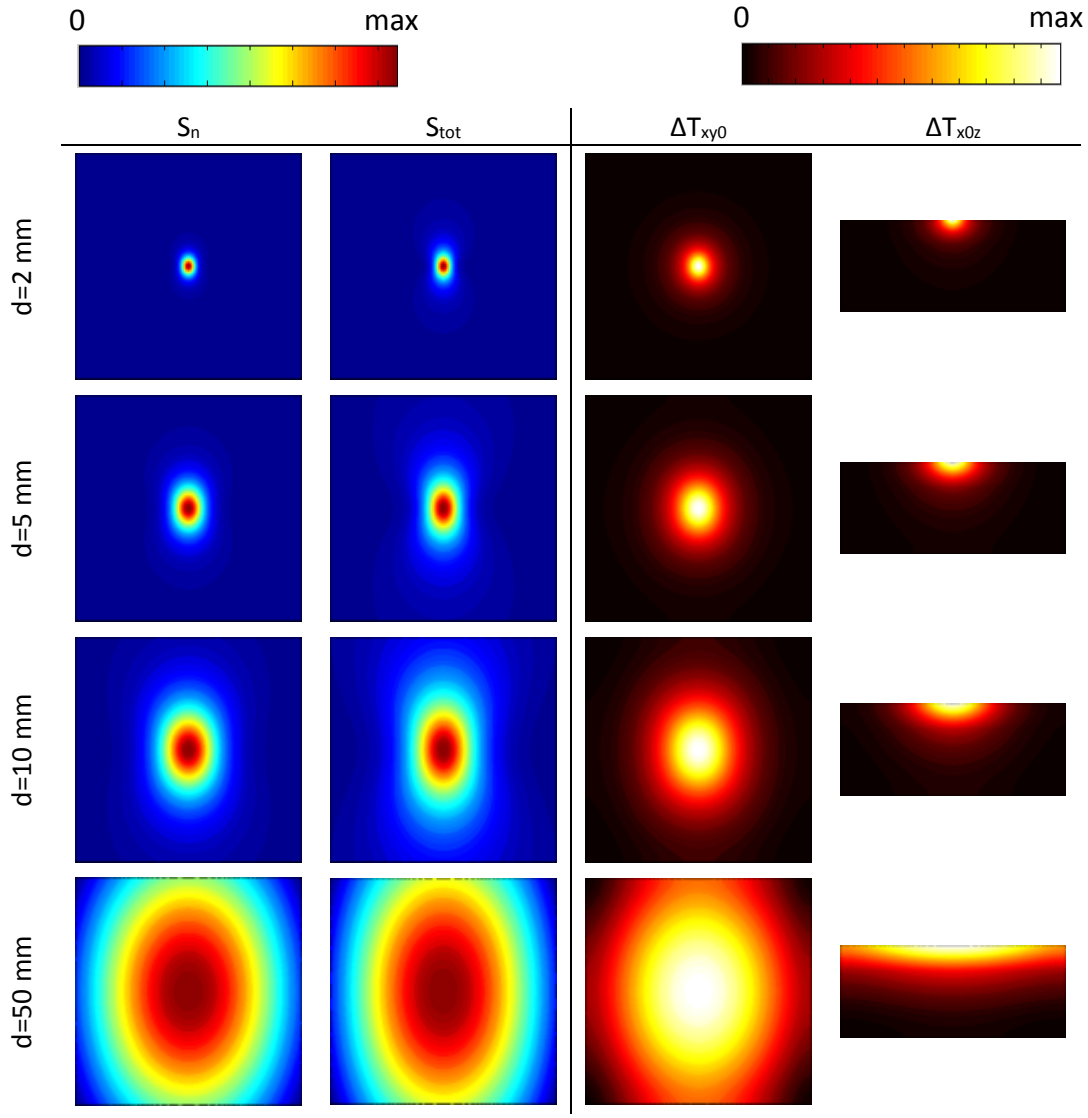

Figure 10: Power density and temperature distribution for the dipole at 90 GHz.

Table 5 The results for the maximum temperature increase (University of Split)

dist [mm]	**freq** [GHz]	**S_n avg. 1cm²** [W/m²]	**S_{tot} avg. 1cm²** [W/m²]	**S_n avg. 4cm²** [W/m²]	**Stot avg. 4cm²** [W/m²]	**ΔT peak** [°C]	**HF_n avg. 1cm²** [°Cm²/W]	**HF_n avg. 4cm²** [°Cm²/W]	**HF_{tot} avg. 1cm²** [°Cm²/W]	**HF_{tot} avg. 4cm²** [°Cm²/W]
2	10	32.826	66.405	12.834	30.733	0.4210	0,013	0,033	0,006	0,014
5		18.503	23.518	8.941	13.734	0.0433	0,002	0,005	0,002	0,003
10		8.462	9.122	5.379	6.561	0.0170	0,002	0,003	0,002	0,003
50		0.518	0.520	0.497	0.503	0.0032	0,006	0,006	0,006	0,006
2	30	39.909	63.311	11.906	22.666	0.1610	0,004	0,014	0,003	0,007
5		21.986	26.567	8.781	12.671	0.1489	0,007	0,017	0,006	0,012
10		9.585	10.263	5.553	6.679	0.0774	0,008	0,014	0,008	0,012
50		0.524	0.526	0.502	0.509	0.0070	0,013	0,014	0,013	0,014
2	60	38.614	59.465	11.352	21.333	0.3471	0,009	0,031	0,006	0,016
5		22.213	26.714	8.687	12.513	0.2281	0,010	0,026	0,009	0,018
10		9.714	10.394	5.565	6.687	0.1044	0,011	0,019	0,010	0,016
50		0.525	0.527	0.503	0.509	0.0088	0,017	0,018	0,017	0,017
2	90	38.122	58.588	11.178	21.047	0.6581	0,017	0,059	0,011	0,031
5		22.248	26.738	8.666	12.483	0.2777	0,012	0,032	0,010	0,022
10		9.739	10.420	5.568	6.689	0.1227	0,013	0,022	0,012	0,018
50		0.525	0.527	0.503	0.510	0.0102	0,019	0,020	0,019	0,020

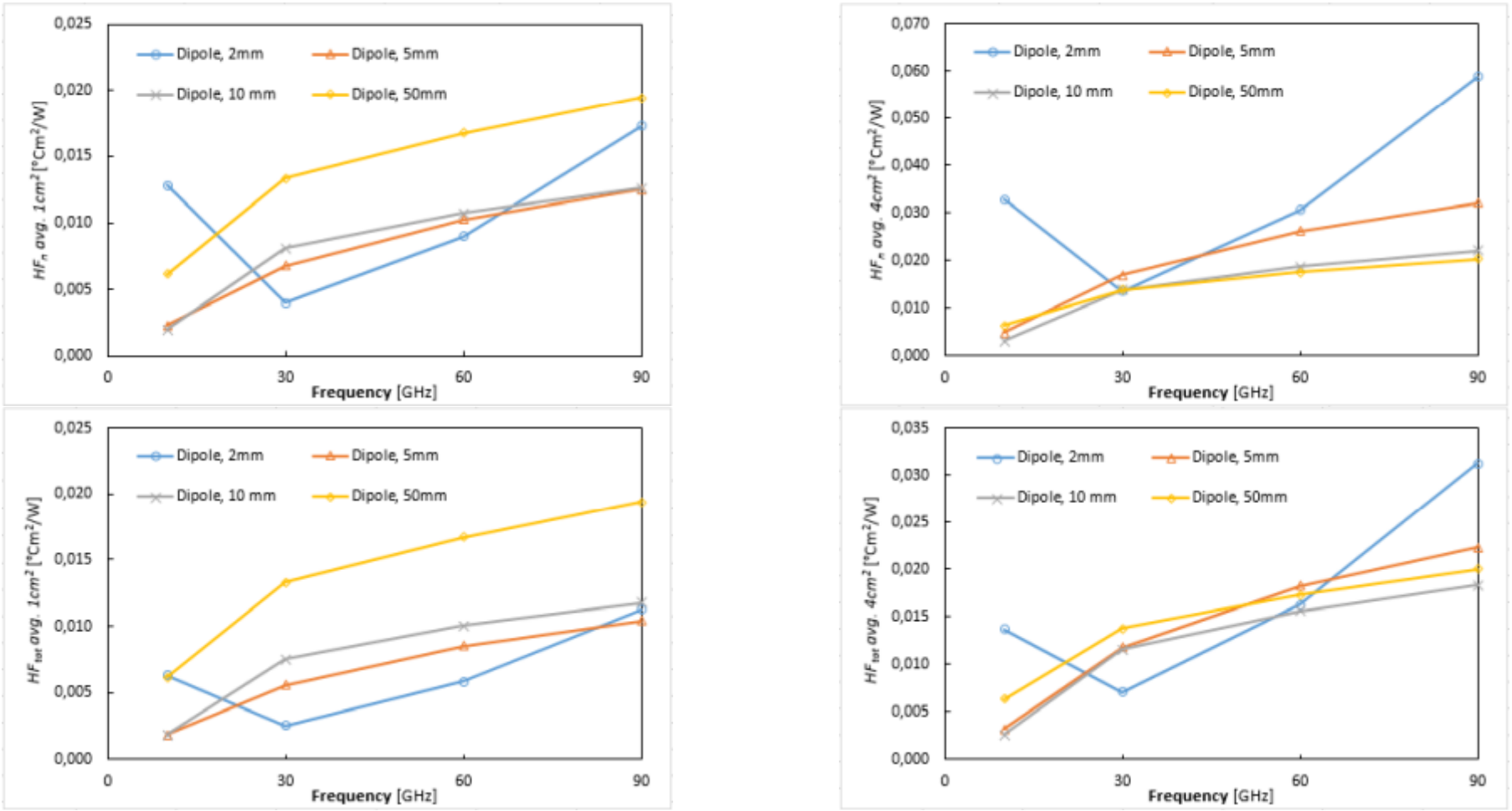

Figure 11: Heating factor comparisons for different averaging area and definition of IPD averaging methods.

Figures 12 to 15 show calculated temperature increase distribution and averaged incident power densities for two averaging methods.